Title
MASS TRANSFER AND TRANSPORT PROPERTIES IN FUSED SALT AND LIQUID METAL SYSTEMS

Authors
Olander, D.R.
Pasternak, A.D.

Publication Date
1969-05-01

Submitted to Nuclear Fuel Reprocessing
Symposium, Ames Laboratory, Ames, Iowa,
August 13-15, 1969

UCRL-19003
Preprint

cy. 2

MASS TRANSFER AND TRANSPORT PROPERTIES IN FUSED SALT AND LIQUID METAL SYSTEMS

D. R. Olander and A. D. Pasternack

May 1969

AEC Contract No. W-7405-eng-48

LAWRENCE RADIATION LABORATORY
UNIVERSITY of CALIFORNIA BERKELEY

DISCLAIMER

Prepared for "Nuclear Fuel Reprocessing Symposium",
Ames Laboratory, August, 1969.

MASS TRANSFER AND TRANSPORT PROPERTIES IN FUSED SALT AND LIQUID METAL SYSTEMS

D.R. Olander
Inorganic Materials Research Division of the
Lawrence Radiation Laboratory and the
Department of Nuclear Engineering of the
University of California, Berkeley, California
and
A.D. Pasternak
Lawrence Radiation Laboratory, Livermore, California

The relevance of fundamental mass transfer studies of high temperature inorganic liquid-liquid extraction systems to the design of pyrochemical reprocessing contactors is discussed. Particular attention is paid to the applicability of theoretical models and correlations developed from low temperature aqueous-organic systems to liquid metals and fused salts. The measurement and prediction of viscosities and diffusivities in liquid metals are reviewed.

I. Studies of Interphase Mass Transfer in Pyrochemical Systems

Development of a practical high temperature fuel reprocessing technique can be divided into three steps:

(1) Demonstration of thermodynamic feasibility
(2) Analysis of the kinetic aspects of the process
(3) Development of appropriate phase contacting devices

Since the beginning of interest in this field in the 1950's, an impressive quantity of information on the chemical and physical equilibria associated with a wide variety of high-temperature non-aqueous systems has been accumulated. As potential processes were identified, work on the development of contacting equipment was initiated(1). While device testing provides some information on the kinetics of the transfer process (e.g., heights of a transfer unit in fused salt-liquid metal packed columns), relatively little work has been performed on the fundamental aspects of mass transfer in non-aqueous systems. This situation is reversed in the broader field of chemical engineering separations in predominantly aqueous systems, where interest in the fundamentals of interphase mass transfer remains high.

Fundamental mass transfer experiments in pyrochemical systems are conducted in devices which offer the best possibility of elucidating each of the stages of the overall transfer process. High transfer rates are not the objective, as they are in the development of an efficient contactor for a practical separation. Instead, mass transfer studies seek to understand the various steps in the overall process, which include transport in the fluid phases and transfer across the phase boundary. The ultimate goal of these studies is to provide a sound basis for predicting transfer rates and the slow step in the interphase transfer process in complex equipment such as mixer-settlers, packed columns or spray towers, which have been considered as potential contactors for pyrochemical reprocessing flow sheets.

Since the types of contactors contemplated for use in high temperature fluid-fluid reprocessing schemes are quite similar to the devices which have been utilized for decades in the chemical separations industry, an important question arises: To what extent can the substantial theoretical information and empirical correlations developed for low temperature aqueous-organic separations technology be applied to high-temperature reprocessing?

There are reasons for suspecting that such information is immediately applicable. Most mass transfer correlations developed for common contactors are couched in terms of dimensionless groups, such as a relation between the Sherwood number (kd/D, where k = mass transfer coefficient, d = characteristic length, D = diffusion coefficient), the Reynolds number and the Schmidt number. Provided only that the fluids involved in the high temperature process are Newtonian (which they are) and no unexpected interfacial reaction occurs, the same correlations should apply equally well at low or high temperatures, to fused salts and liquid metals as well as to water and organic solvents.

There are, however, valid reasons for questioning the applicability of information obtained from low temperature aqueous-organic systems to high temperature inorganic systems. Applying correlations developed for the former to the latter systems often requires extending the correlation far beyond the range for which it was empirically determined. For example, the density differences and interfacial tensions between immiscible liquid metals may be as much as an order of magnitude greater than any aqueous-organic system. Such a direct extension of heat transfer correlations of ordinary fluids in pipes to liquid metal heat transfer, for example, is invalid because of the very low Prandtl numbers of liquid metals.

Furthermore, although interfacial resistance is rarely important in clean aqueous-organic solvent extraction, the radically different chemical nature of the phases in liquid metal-fused salt systems may be more conducive to interfacial resistance, just as many studies of liquid metal heat transfer have shown evidence of an anamalous resistance at the liquid-solid boundary.

Consequently, our object here is to review some of the experimental studies of interphase mass transfer in high temperature inorganic systems, in order to determine whether such systems present unique problems, or whether they can be considered simply as extensions of aqueous-organic systems. We will consider transfer between two immiscible liquid phases exclusively, emphasizing extraction between two liquid metals and liquid metal-fused salt extraction. The kinetics of gas-solid reactions, which are important in fluidized bed reprocessing or gas-fused salt systems important in some volatility processes, will not be treated.

Mass transfer between solid metals and liquid metals appears to follow the same patterns as ordinary fluid-solid systems. Dunn et al(2) have studied natural convective mass transfer of tin, cadmium, zinc and lead cylinders into mercury and forced convection mass transfer of zinc from the walls of zinc tubes into flowing mercury. Kassner(3) has shown that the dissolution rate of a rotating disk of tantalum into liquid tin is fluid diffusion controlled and that the rate can be predicted from the solutions of the flow and diffusion equations for this geometry.

Interphase Mass Transfer Between High Temperature Immiscible Liquids

Theory

In the absence of a resistance at the phase boundary, mass transfer between immiscible liquid phases is governed by the transfer coefficients in each phase and the thermodynamic equilibrium conditions at the interface. In keeping with the objectives of fundamental studies of the mass transfer process, it is important that the contacting methods permit theoretical or empirical estimation of the diffusional resistances in each phase for comparison with experiment. It must be possible to establish the expected diffusion controlled rate, since any deviation of the experimental results may be an indication of an interfacial resistance.

Studies of this type in aqueous-organic systems can be conducted with relatively complex equipment, in order to allow precise calculation of the individual film resistances. Such devices include laminar jets of one liquid in another, co-current stratified flow of the two liquids in a duct, or wetted wall columns in which the central fluid is liquid. With fused salts and liquid metals at temperatures in excess of 500°C, however, the experimental problems involved in using sophisticated contacting devices are insurmountable. Consequently, all studies of liquid-liquid extraction kinetics in high temperature inorganic systems have utilized the classic method of falling drops.

There is an extensive literature on the theory and measurement of the mass transfer coefficients outside of falling drops (the external coefficient) and on the inside of the drop (the internal coefficient) to which the high temperature experimental results can be compared.

Sideman and Shabtai(4) summarize thirty different correlations that have been employed for the analysis of external mass transfer in drop extraction. These correlations can be divided into those based upon assumption of a rigid drop and those based upon internal circulation within the drop.

The rigid drop models are extensions of the theory of transfer from a solid sphere, and lead to Sherwood number relations of the form:

$$Sh_e = 2 + bSc_e^{1/3}\sqrt{Re_e} \qquad (1)$$

$$Sh_e = \frac{k_e d}{D_e} \qquad \text{Sherwood number} \qquad (2)$$

$$Sc_e = \nu_e/D_e \qquad \text{Schmidt number} \qquad (3)$$

$$Re_e = du/\nu_e \qquad \text{Reynolds number} \qquad (4)$$

k_e is the external mass transfer coefficient (cm/sec), d the drop diameter, D_e the diffusion coefficient of the transferring solute in the external (continuous) phase, ν_e the kinematic viscosity of the continuous phase and u the fall (or rise) velocity of the drop.

The constant term "2" on the right of Eq(1) represents the steady state rate of molecular diffusion in an infinite stagnant liquid surrounding the drop. The second term in Eq(1) accounts for the increased transfer rate due to the boundary layer (or "film") generated by the motion of the drop past the surrounding liquid. Although the coefficient b has been found to vary from 0.4 to 0.9, values in the vicinity of 0.6 are most common.

Circulation within the drop increases transfer rates by reducing the external boundary layer. In the limit of no external boundary layer, the velocity field external to the drop can be approximated by potential flow and the resulting Sherwood number is given by:

$$Sh_e = \frac{2}{\sqrt{\pi}}\sqrt{Sc_e Re_e} = 2\left(\frac{D_e u}{\pi d}\right)^{1/2} \qquad (5)$$

Eq(5) is identical to Higbie's penetration theory(5) (unsteady state diffusion into the fluid adjacent to the drop) if the contact time is considered as the time required for the drop to fall one diameter.

Models of internal transfer which have been employed in aqueous-organic drop extraction studies are based on stagnant diffusion(6), internal circulation(7), a type of eddy diffusion(8), and explicit recognition of drop oscillation(9,10). Of these, the Handlos-Baron eddy diffusion model has been used most extensively. The original theoretical treatment of this model yielded:

$$Sh_i = 0.00375 \frac{Re_i Sc_i}{1 + \mu_i/\mu_e} \qquad (6)$$

$$Sh_i = k_i d/D_i \qquad (7)$$

$$Sc_i = \nu_i/D_i \qquad (8)$$

$$Re_i = du/\nu_i \qquad (9)$$

The subscript i denotes properties of the drop and μ is the absolute viscosity. Several modifications of Eq(6), required to rectify some mathematical deficiencies of the model, have been developed by Olander$^{(11)}$ and Patel and Wellek$^{(12)}$.

The stagnant drop model of internal mass transfer utilizes the solution of the molecular diffusion equation in a sphere. Transient solutions of this type do not yield an internal mass transfer coefficient directly. Instead, the fraction of the solute initially present in the drop which has been removed is specified as a function of contact time. The fraction extracted is related to the internal mass transfer coefficient by:

$$k_i = - \frac{d}{6t} \ln(1-f) \qquad (10)$$

where f is the fraction extracted and t is the contact time. For the solution of the stagnant diffusion model by Newman$^{(6)}$, the fraction extracted is:

$$f = 1 - \frac{6}{\pi^2} \sum_{n=1}^{\infty} \frac{1}{n^2} \exp\,[-n^2\pi^2\tau] \qquad (11)$$

where τ is a dimensionless contact time, defined by:

$$\tau = \frac{4D_i t}{d^2} \qquad (12)$$

Eq(11) is inconvenient to use when the contact time is short because many terms of the sum are needed. The alternate expression:

$$f = \frac{6}{\sqrt{\pi}} \sqrt{\tau} - 3\tau \qquad (13)$$

is satisfactory for nearly all applications of this model to extraction data. Because of the explicit dependence of the mass transfer coefficient on contact time in the stagnant drop model, the concept of a mass transfer coefficient loses some of its convenience.

For extraction systems in which external and internal resistances are important, the transfer rate is controlled by the overall mass transfer coefficient:

$$\frac{1}{K} = \frac{1}{k_i} + \frac{1}{mk_e} \tag{14}$$

where m is the equilibrium ratio of the solute concentration on the external phase side of the interface to the concentration on the drop side of the interface. This relation is useful only if the quantity m is independent of concentration.

Interfacial Equilibrium

If there are no extraneous resistances at the phase boundary, the concentrations of the transferring solute on the two sides are fixed by thermodynamic considerations. Three types of interfacial equilibria have been investigated in high temperature extraction systems.

1) Physical Equilibrium. When the two phases are immiscible liquid metals, the coefficient m in Eq(14) is the equilibrium distribution coefficient of the transferring solute between the two solvent metals. If the diffusing species is solvent 1 transferring to an immiscible liquid 2 which is unsaturated with respect to liquid 1, the coefficient m is the solubility of 1 in 2.

2) Chemical Equilibrium. In fused salt-liquid metal transfer, the metal phase generally contains a solute metal which can be oxidized by an extracting agent B^{+n} in the salt phase. Equilibrium at the interface is governed by the law of mass action applied to the exchange reaction:

$$S_i(m) + B_i^{+n}(s) = B_i(m) + S_i^{+n}(s) \tag{15}$$

for which

$$K_{eq} = \frac{B_i S_i^{+n}}{S_i B_i^{+n}} \tag{16}$$

For simplicity, the valences of the two cations S and B have been taken to be equal. The concentrations in Eq(16) have been written in terms of molar concentrations, since these are the appropriate units for describing the diffusional transfer step. The subscript i denotes a value at the phase boundary. The activity coefficient ratios which normally appear on the right hand side of Eq(16) have been assumed constant and incorporated into the equilibrium constant.

The simple overall mass transfer coefficient concept of Eq(14) is inconvenient to use in the present case, since Eq(16) renders the interfacial equilibrium condition non-linear. Instead, it is easier to relate the parameters of the problem (initial concentration, equilibrium constant and mass transfer coefficients) directly to the fraction of the solute extracted from the drop phase. Generally, the metal phase is dispersed in the continuous salt phase. A metal drop falling through the salt will at all times be exposed to the same concentration of extractant in the salt, or B^{+n} = constant. The concentration of the solute in the drop decreases from an initial value of S_o to some value S while the product metal in the bulk of the drop increases from zero to B. Since this particular exchange reaction is equimolar, $S_o = S+B$. Typical concentration profiles near the interface are depicted schematically in Fig. 1.

The individual film mass transfer coefficients are defined in terms of the molar fluxes per unit interfacial area and the molar concentration driving forces:

$$N_B = k_e^B(B^{+n}-B_i^{+n}) = k_i^B(B_i-B) \tag{17}$$

$$N_S = k_e^S S_i^{+n} = k_i^S(S-S_i) \tag{18}$$

For the reaction stoichiometry considered in this example, $N_B = N_S = N$. The mass transfer coefficients of the two species in a given phase differ only if the diffusion coefficients differ. Since the mass transfer coefficients vary approximately as the square root or the 2/3 power of the diffusion coefficient, and since the diffusivities of similar species in the same solvent are nearly equal, it is appropriate to make the approximations:

$$k_e^B = k_e^S = k_e \quad \text{and} \quad k_i^B = k_i^S = k_i \; .$$

Eqs(16), (17), and (18) must be solved simultaneously to eliminate all interfacial concentrations and to obtain an expression for the flux N in terms of the bulk concentrations S, S_o, and B^{+n}, the mass transfer coefficients k_e and k_i, and the equilibrium constant K_{eq}. In general, the flux depends upon the concentration S in a non-linear manner.

A significant simplification in the analysis with exchange occurs if the equilibrium constant of Eq(16) is very large (this situation is usually called an "irreversible" reaction in the literature on mass transfer with chemical reaction). If $K_{eq} \rightarrow \infty$, either S_i or B_i^{+n} must be zero. If $S_i \rightarrow 0$, Eq(18) indicates that the flux is given by $N = k_i S$, which is the condition of transfer completely controlled by resistance within the drop. On the other hand, if $B_i^{+n} \rightarrow 0$, transfer is controlled completely by diffusion in the salt phase, and by Eq(17), $N = k_e B^{+n}$. The actual controlling mechanism is the one which yields the smaller rate. In a drop extraction experiment, where the concentration in the metal drop S decreases with contact time, the rate may be controlled by external transfer in the top of the column and by internal transfer at the end of fall. The two mechanisms participate in the determination of the amount extracted in a consecutive fashion instead of by the series manner implied in the overall coefficient of Eq(14).

If K_{eq} is finite, Eqs(16) - (18) can be solved for S_i^{+n} which is determined by solution of:

$$(K_{eq}-1)\gamma(S_i^{+n})^2 - [K_{eq}(\gamma B^{+n}+S) + (S_o-S)](S_i^{+n}) + K_{eq}SB^{+n} = 0 \qquad (19)$$

where γ is the ratio k_e/k_i.

The decrease in the concentration of the solute in the metal phase as the drop falls through the salt is given by the material balance:

$$\frac{dS}{dt} = -\frac{6}{d}N \qquad (20)$$

With $N = k_e(S_i^{+n})$ from Eq(18), the concentration S after a contact time t is determined from:

$$\int_{S_o}^{S} \frac{dS}{(S_i^{+n})} = -\frac{6k_e}{d}t \qquad (21)$$

where S_i^{+n} is the solution of Eq(19). In general, the integral on the left of Eq(21) cannot be performed analytically. The quantity usually measured in the experiment is the fraction of the solute extracted from the drop after falling through a length L of salt:

$$f = 1 - S/S_o \tag{22}$$

where the contact time is $t = L/u$.

If the internal resistance to mass transfer is negligible ($\gamma = 0$), Eq(19) can be solved. The fraction extracted is given by:

$$-\ln(1-f) + (K_{eq}-1)f = \frac{6t}{d}K_{eq}k_e\left(\frac{B^{+n}}{S_o}\right) \tag{23}$$

3) <u>Isotopic Equilibrium</u>. If the species S and B in the salt-metal exchange reaction are isotopes of the same metal species, the equilibrium constant of Eq(16) is identically unity. Eq(19) can be solved and the flux written as:

$$N = \left[\frac{k_e(B^{+n}/S_o)}{1+(B^{+n}/S_o)\gamma}\right]S \tag{24}$$

The bracketed term in this expression is an overall mass transfer coefficient of the type given by Eq(14). The "distribution coefficient" m is identified with the concentration ratio (B^{+n}/S_o). Isotope exchange has the capability of covering the entire range from complete internal control to complete external control simply by adjusting the ratio (B^{+n}/S_o).

Slow Interfacial Chemical Reaction

If the chemical exchange reaction, Eq(15), proceeds at a rate comparable to the diffusion rates, equilibrium between the two phases at the interface cannot be attained. If the chemical reaction mechanism is the same as the overall reaction, the interface condition of Eq(16) is replaced by:

$$N = k_r\left(B_i S_i^{+n} - \frac{1}{K_{eq}} S_i B_i^{+n}\right) \tag{25}$$

Eq(16) is seen to be a special case of Eq(25) which is approached as the chemical rate constant k_r becomes very large.

Drop Fall Velocity

In order to determine the contact time in a drop extraction process, the fall velocity of the drop must be known. These velocities have rarely been measured in high temperature systems, and the fall velocity is usually computed by assuming that the Hu-Kintner correlation(14), which was developed for aqueous-organic systems, applies.

Comparison With Experiment

Drop extraction experiments provide information on the variation of the fraction extracted f for variations of the controllable parameters d (drop diameter), t (contact time, varied by adjusting the height of the salt column) and in chemical or isotopic exchange experiments, by altering the concentration ratio (B^{+n}/S_o). Generally the temperature is maintained constant at some convenient value. The experimental results are compared to a theoretical model such as one of those discussed above. Lack of agreement between theory and experiment can be attributed to one of the following reasons:

1) The theoretical or empirical expressions for k_i or k_e (usually taken from investigations of aqueous-organic systems) do not apply to the high temperature system.

2) A slow chemical step occurs at the interface (i.e., k_r of Eq(25) is not very large.

3) There is an additional resistance at the interface, due perhaps to impurities (lack of intimate phase contact due to non-wetting is very unusual in liquid-liquid systems).

4) Even if equilibrium prevails at the interface, the dynamic data (K_{eq} or m) upon which the interface condition is based are in error.

5) The transport properties may not have been measured or are poorly estimated from correlations.

A review of several experiments on high temperature liquid-liquid extraction will indicate the degree with which such experiments agree with drop extraction theory.

Drop Extraction Experiments

The first experiments specifically designed to investigate the kinetics of drop extraction with high temperature reprocessing in view were those reported by Bonilla at the First Geneva Conference(15).

To minimize the problems associated with containing reactive metals at elevated temperatures, the lead-zinc system was studied at 450°C. The two partially miscible solvents were initially free of the other component. The sealed pyrex tube containing the two solvents was brought to temperature in the position shown by the solid diagram in Fig. 2. The tube was then tilted by 105° so that the lead fell through the zinc and the zinc rose to the top. After rapid solidification, the concentrations of zinc in the lead and lead in the zinc were measured. It was hoped that the zinc would rise through the lead as a single large drop, thus permitting comparison of the external mass transfer coefficient in the lead phase and the internal coefficient in the zinc drop with drop extraction theory. However, the measured external coefficient was 30 times greater than the value computed from Eq(5), probably because the zinc phase had broken up into many small drops instead of rising as a single sphere.

Internal coefficients in a fused salt-liquid metal extraction were measured by Bonilla in the drop rise experiment shown in Fig. 3. The LiCl-KCl eutectic contained in compartment A of the pyrex apparatus was fed by inert gas pressure through tube E into the cadmium resevoir B. By forcing the salt through nozzle C, drops of 3 mm diameter were produced. Since cadmium is slightly soluble in the salt, but the salt is insoluble in cadmium, only cadmium transfer into the salt drops occurred. The mass transfer coefficient inside the salt drops was obtained from the terminal cadmium concentrations in the collected salt. However, the data were compared to the predictions of the Higbie model (which applies to external mass transfer) rather than to one of the internal mass transfer models.

The first salt-metal kinetic experiment which considered an exchange reaction at the interface was reported by Katz, Hill, and Speirs in 1960(16). They studied the transfer of Sm from a bismuth phase to a NaCl-KCl-$MgCl_2$ salt phase by the Sm-$MgCl_2$ exchange reaction. Metal drops of 2.2 mm diameter were introduced into the salt phase in the Vycor device shown in Fig. 4. Smooth drop entry was accomplished by moving the notch in the central rod up to the bismuth reservoir in the upper compartment, then lowering the rod into the salt phase so that the small amount of metal contained in the notch fell through the salt. In order to minimize the continued extraction from the puddle of metal at the bottom of the column, the constriction shown in the bottom of the apparatus was provided to reduce diffusion to and from the collected metal. The fraction extracted was determined by analysis of the salt after 15 drops had been released in this fashion. The contact time was varied by using salt columns varying from 7 to 25 cm in height. Because the equilibrium constant strongly favored accumulation of samarium in the salt phase (equivalent to a large value of m in Eq(14)), external resistance to mass transfer was small compared to resistance within the falling drop. The extraction rates were satisfactorily represented by the Handlos-Baron internal mass transfer coefficients (Eq(6)).

Both chemical and isotopic exchange in a fused salt-liquid metal system were investigated by Olander(17). Chemical exchange involved extraction of zinc from a zinc-lead alloy by reaction with lead chloride in the LiCl-KCl eutectic:

$$\mathrm{Zn(m)} + \mathrm{Pb}^{+2}\mathrm{(s)} = \mathrm{Pb(m)} + \mathrm{Zn}^{+2}\mathrm{(s)} \qquad (26)$$

The apparatus used is shown in Fig. 5. Metal drops of diameters ranging from 1 to 5 mm were introduced into the top of the column. As in the experiments of Katz et al(16), precautions were taken to minimize extraction during drop entry and after drop fall had been completed. Elimination of these end effects is essential if the extraction data are to be compared to the theoretical models described previously, all of which are based upon mass transfer only during free fall of the drop.

Mass transfer during introduction of the drop into the salt was minimized (but not eliminated) by using one of the two entry techniques shown in Fig. 6. In the rod entry method, the drop was speared on the tip of a pyrex rod and lowered into a layer of solute-free salt which had been carefully poured on top of the extracting salt in the column. In the dropper entry method, drop fall was initiated by removing the plunger from the funnel stem shown in Fig. 6b. The molten metal pellet then fell first through a solute free layer and then into the extracting salt.

Reduction of the bottom end effect was accomplished in the following manner. Just prior to drop release, the temperature at the bottom of the salt column was reduced below the freezing point of the salt. The falling drop encountered an advancing solidification front as it reached the end of its fall, and continued extraction was prevented by enveloping the drop in solid salt.

Isotope exchange was studied by replacing lead chloride in the salt phase by zinc chloride. The tracer zinc-65 in the metal phase exchanged with natural zinc in the salt phase.

The fractions extracted were the same for both chemical and isotopic exchange, and both varied linearly with the ratio of the concentration of extractant in the salt to the concentration of zinc in the metal. These two observations suggested complete control of the extraction process by external (salt phase) mass transfer. The external mass transfer coefficients obtained from the data were in rough accord with those predicted by the rigid drop model (Eq(1)).

There were indications that the mechanism of the interfacial reaction did not follow the overall reaction of Eq(26) for all conditions. When pure zinc drops were contacted with lead chloride solutions, the recovered drop was partially encased by a black crust, which consisted primarily of tiny spheres of metal. It was hypothesized that the primary rapid reaction at the interface was:

$$Pb^{+2}(s) + 2Zn(m) = Pb(m) + Zn_2^{+2}(s) \tag{27}$$

The zinc subchloride begins diffusing towards the bulk of the salt but produces finely dispersed metal particles in the boundary layer by one of the following reactions:

$$Zn_2^{+2}(s) = Zn\downarrow + Zn^{+2}(s) \tag{28}$$

or

$$Zn_2^{+2}(s) + Pb^{+2}(s) = Pb\downarrow + 2Zn^{+2}(s) \tag{29}$$

This model predicts that when interfacial reaction is governed by Eq(27) rather than by Eq(26), twice as much zinc should be extracted for the same lead chloride bulk concentration (since each Pb^{+2} reaching the metal drop moves two zinc atoms by reaction (27) but only one by reaction (26)). This feature of the subchloride model was qualitatively confirmed by the extraction data.

The results for this system suggested that a number of forms of rate-enhancing interfacial turbulence, which have also been observed in aqueous-organic systems, may be important in high temperature inorganic systems as well. Drop oscillation was observed, and some experiments suggested accelerated transfer due to a Marangoni-type interfacial motion.

Mass transfer and drop fall velocities were measured in an immiscible liquid metal extraction system by Pasternak and Olander(18). Lanthanum-140 and barium 140 were transferred from 2-4 mm diameter drops of the uraniumchromium eutectic alloy freely falling through a column of molten magnesium at 1000°C. The all-graphite extraction column shown in Fig. 7 was employed. At this temperature (which is 500°C higher than the three salt-metal experiments discussed above), not even the modest refinements in drop entry methods used in the salt-metal studies were feasible. The reactor-irradiated U-Cr drop was simply suspended from a tungsten wire and lowered into the molten magnesium. After melting, it detached from the wire and fell through the column. The progress of the drop down the column was followed by the response of three collimated scintillation detectors placed at intervals along the length of the column. To minimize continued extraction before the system was frozen after an experiment, a puddle of molten $BaCl_2$ was placed at the bottom of the column to receive the falling drop and remove it from direct contact with the magnesium extractant.

The drop terminal velocities measured from the responses of the three detectors were in good agreement (15%) with the Hu-Kintner relation(14), despite density differences, interfacial tension, and viscosities far beyond the range of this aqueous-organic based correlation.

Mass transfer coefficients of lanthanum were measured directly by determination of La-140 activity pick-up in the magnesium ingot. By following the decay of the La-140 activity in the ingot for about three weeks after the experiment and utilizing the radiochemical decay properties of the two member Ba-140-La-140 chain, the mass transfer coefficient of barium was determined as well.

Since the distribution coefficient (Mg-to-U-Cr) of lanthanum was approximately 50 times that of barium, lanthanum extraction was expected to be controlled by transport within the drop and barium extraction by transfer in the external magnesium phase. These predicitions were borne out by the data. To within the precision of the data, lanthanum extraction followed the stagnant diffusion model of internal transfer (Eq(13)), while barium transfer agreed with the Higbie model.

Conclusions

Because of the rather forbidding array of problems associated with working with reactive liquid metals at elevated temperatures, very few high temperature (>500°C) liquid-liquid extraction experiments have been performed. Equilibrium measurements with the same systems of course encounter identical stringent restrictions on container materials and system cleanliness, but the kinetic experiments have the additional requirement of moving one phase relative to the other in a manner which permits theoretical determination of the flow patterns and hence the mass transfer coefficients. In addition, the kinetic experiments require reliable equilibrium data (in the form of distribution coefficients, solubilities, or two-phase equilibrium constants) in order to interpret the extraction data. Often, the lack of good thermodynamic or transport property data may be the greatest impediment to obtaining reliable mass transfer information. Where such data are available, the mass transfer studies have shown that the liquid metal-fused salt extraction kinetics are adequately described by one of the many mass transfer correlations developed for low temperature aqueous-organic systems. The extension of these empirical correlations for physical properties and temperatures far beyond the range in which they were developed appears justified.

Although aqueous-organic correlations appear to adequately describe the results of the relatively crude high temperature kinetic measurements, there is no agreement as to which correlation is applicable for a particular set of conditions. For example, the metal phase internal coefficients determined by Katz et al(16) fit the Handlos-Baron model, while Pasternak and Olander(18) found that the metal phase transfer coefficients agreed best with the stagnant diffusion model. The applicability of these two models (which differ quantitatively by a factor of five under these conditions) may depend upon the nature of the external phase; in the former, the continuous phase was a fused salt while in the latter, it was another liquid metal. As another example, the salt-metal experiments of reference 17 showed external transfer coefficients comparable to those expected for a rigid drop, yet the external coefficients determined by the metal-metal experiments of reference 18 were of the order expected from the Higbie model. These two models predict external coefficient an order of magnitude apart.

Retardation of mass transfer due to interfacial resistance has not been observed in any experiments. If slow chemical reaction is the form of interface resistance, this observation is not surprising. Chemical rate constants increase much more rapidly with temperature than mass transfer coefficients, and one would have to search diligently for a reaction between two fluid phases which was slower than diffusion in the temperature range from 500-1000°C.

It is somewhat surprising, however, that inhibition of extraction due to interface-seeking impurities have not been reported, particularly since these effects have been reported in aqueous-organic systems. Since most liquid metals at these temperatures will react readily with impurities in the cover gas, in the solvent phases proper, or with the container material, there should have been a much more severe contamination problem than in relatively non-reactive low temperature aqueous-organic systems.

The mass transfer studies of high temperature liquid-liquid systems have not yet demonstrated unequivocally that prediction methods based upon experience with aqueous-organic systems are directly applicable to pyrochemical reprocessing systems. They have shown, however, that for devices such as spray columns and mixer settlers, the liquid metal-fused salt and immiscible liquid metal results at least fall in the range of the common aqueous-organic correlations. So far, no rate-limiting phenomena peculiar to high temperature inorganic species have been uncovered. However, problems unique to liquid metals may appear in other contacting devices such as packed columns where phase contact involves a third solid phase. In this case, the degree of wetting of the packing by one or both of the immiscible liquid phases may be important.

II. Transport Properties of Liquid Metals

Interpretation of mass transfer experiments in liquid metal-fused salt systems requires a knowledge of solvent viscosities and solute diffusivities. The dimensionless Sherwood, Schmidt, and Reynolds numbers, which are used to correlate mass transfer coefficients, depend upon these transport properties. In order to apply the correlations, measurements or estimates of viscosity and diffusivity for the particular system of interest are required.

In recent years, considerable effort has been devoted to measuring the viscosity of pure liquid metals and liquid metal alloys and also to the measurement of diffusion coefficients in liquid metal systems. Many of these experiments have been on systems of particular importance in nuclear reactor and pyrochemical fuel processing technology.

In addition to experimental measurements, methods for estimating viscosities and diffusivities have been develooped. These methods involve semi-empirical correlations in which the value of an adjustible parameter is determined by the existing data. Assuming that liquid metals all show similar behavior with respect to the adjustible parameter, the correlation can then be applied to systems for which data are not yet available.

Viscosity Correlations

Two methods for estimating liquid metal viscosities are those of Grosse(19) and Chapman(20). Grosse's method assumes an exponential dependence of viscosity on temperature:

$$\eta = a \exp \left[H_\eta / RT\right] \tag{30}$$

where η is the viscosity in poises, H_η is the activation energy of viscous flow in cal/g-atom, R is the gas constant in cal/g-atom-°K, and T is the absolute temperature in °K. Andrade's expression(21,22), is used to estimate viscosity at the melting point.

$$\eta_m = 5.7 \times 10^{-4} \frac{\left(AT_m\right)^{1/2}}{V^{2/3}} \tag{31}$$

where A is the atomic weight, T_m the melting point, and V is the atomic volume at the melting point in cc/g-atom. Grosse finds the following empirical correlation between

H_η and the melting point, T_m.

$$\log_{10}H_\eta = 1.348\log_{10}T_m - 0.366 \qquad (32)$$

From Eqs(31) and (32), the pre-exponential factor, a, in (30) can be determined. Eq(30) can then be used to estimate viscosity over the entire liquid range.

Chapman(20) uses the radial distribution function concept of the liquid state to establish a functional relationship between reduced viscosity, reduced volume, and reduced temperature. These quantities are reduced with a distance parameter (the Goldschmidt atomic diameter) and an energy parameter. Energy parameters for the liquid metals are empirically found to be about $5.2kT_m$. Grosse's correlation requires the molecular weight, melting point, and density at the melting point; Chapman's correlation requires the molecular weight, melting point, density over the temperature range of interest, and Goldschmidt atomic diameter.

Viscosities of the Actinides

The only experimental determination of the viscosity of plutonium is that of Jones, Ofte, Rohr and Wittenberg(23) whose measurements cover the range from 645-950°C. Ofte(24) has also measured the viscosity of uranium contained in sub-stoichiometric zirconia crucibles from 1141-1248°C. The viscosity of uranium has also been measured recently by Finucane and Olander(25) in both tantalum and beryllia crucibles. Their measurements cover the range from the melting point to 1532°C. All of these measurements employ the oscillating crucible technique, which is an absolute method requiring no calibration with a liquid of known viscosity. The data for these three measurements are shown in Figure 8 along with values predicted by the Grosse and Chapman correlations. All of the measured viscosities are higher than the predicted values, and it may be that the actinide metals behave as a class apart from other metals.

The data of Finucane and Olander for uranium show greater precision over a wider temperature range than do those of Ofte. However, the $\sim$ 35% discrepancy between the two sets of data will have to be resolved by a third measurement.

Viscosities of the Rare Earths

Viscosities and densities of the molten rare earths lanthanum, cerium and praseodymium have been measured by

Wittenberg, Ofte and Rohr(26,27) in the temperature range from the melting point to over 1000°C. Figure 9 compares the data with Grosse's and Chapman's correlations. Both correlations fall within the scatter of experimental data for all three metals. It should be noted, however, that the activation energy from the least squares fit is much smaller than that predicted by either of the two correlations. Therefore, extrapolation of the data to higher temperatures may involve considerable error.

Viscosities of Plutonium Alloys

Since the early 1960's, the viscosities of several plutonium alloys have been measured at the Mound Laboratory. These alloy systems are Pu-Ce-Co(23), Pu-Ce(28), Pu-Fe(29), Pu-U(30) and Pu-Ga(30). These alloys are of interest as possible reactor liquid fuels. In all cases, the addition of alloying elements to plutonium produces a viscosity increase. The effect is most pronounced in the case of Ga where a 3.3 atom percent addition causes a 50% rise above the viscosity for pure plutonium. In the Pu-U system, there is a relative viscosity maximum, apparent in all isotherms up to 800°C, at a composition of 10.8 atomic percent uranium. This is the composition of the lowest melting alloy in the system, 620°C. Viscosity isotherms for the Pu-Fe system show a maximum at the eutectic composition of 9.5 atomic percent iron. Viscosity isotherms for the Pu-Ce system are the most unusual of all. Additions of Ce produce a rise in viscosity to a maximum at 5 atomic percent cerium. Viscosity then decreases to a minimum at 14 atomic percent cerium followed by a slight rise at the eutectic composition, 16.5 atomic percent cerium. There is no theory to adequately explain or predict the wide variety of viscosity behavior in liquid metal alloys. Some systems show a viscosity minimum at the eutectic point. For such a frequently studied system as the lead-tin pair there is disagreement in the literature. Fisher and Phillips(32) observe a viscosity minimum at the eutectic point; Kanda and Colburn(33) observe linear viscosity isotherms over the complete composition range from pure tin to pure lead. Some Russian investigators have applied thermodynamic (heat of mixing) data to the study of alloy viscosity behavior. Burylev(34) has shown a relationship between viscosity isotherms for Cu-Ag alloys (which have a minimum) and thermodynamic data. Eretnov and Lyubimov(35) have investigated the relationship between viscosity isotherms for several copper alloy systems which have maxima and heat of mixing data, while for other systems(36) volume changes on mixing are more important.

Diffusivity Correlations

Mutual diffusion coefficients in a number of dilute liquid metal solutions have been correlated by Pasternak and Olander(37) using a modified form of absolute rate theory. The theory was developed by Olander(38) to correlate mutual diffusion data in dilute organic systems, and uses viscosity data for both pure solvent and pure solute to estimate the difference between the free energies of activation of the viscous and diffusive processes. The correlation for liquid metals is shown in Figure 10; the dashed lines represent 25% deviation from the best line. The dimensionless group Y and the parameter f are defined by:

$$Y = \left(\frac{d\eta}{T}\right)\left(\frac{5.31}{k}\right)\left(\frac{V}{N}\right)^{1/3} = \exp\,[0.5\delta] \qquad (32)$$

$$\delta = \left(\frac{\Delta F^*_{AA}}{RT}\right)\left[1-\left(\frac{\Delta F^*_{BB}}{\Delta F^*_{AA}}\right)^{1/2}\right] \qquad (33)$$

where k is the Boltzmann constant, N is Avogadro's number, and ΔF^*_{AA} and ΔF^*_{BB} are the free energies of activation for viscosity for pure solvent and pure solute respectively. Free energies of activation are obtained from viscosity data by the expression

$$\eta = \frac{Nh}{V}\exp\,[\Delta F^*/RT] \qquad (34)$$

where h is Planck's constant.

For systems where the diffusing solute is a solid at the temperature of measurement, ΔF^*_{BB} is obtained by a linear extrapolation of ΔF^*_{BB} values obtained in the liquid region according to:

$$\Delta F^* = \Delta H^* - T\Delta S^* \qquad (35)$$

where ΔH^* and ΔS^* are the entholpy and entropy of activation of viscosity obtained for pure solute metal above its melting point.

Liquid metal diffusion coefficients have often been estimated by the Stokes-Einstein equation:

$$D = \frac{kT}{6\pi r\eta} \qquad (36)$$

where r is a characteristic radius of the diffusing solute atom. The Stokes-Einstein equation is based on a hydrodynamic model of a large solute atom moving through a continuous fluid with a "no-slip" condition at the solute atom surface. For liquid metals, the size parameter r in Eq(37) is usually taken as the ionic rather than the atomic radius of the solute atom. Based on a study of viscosities in liquid metals, Eyring(39) concludes that the unit of flow is probably the metal ion stripped of its valence electrons.

For self-diffusion, $\delta=0$ and $Y=1$ in Eqs(32) and (33). Therefore, if the self-diffusion coefficient for the pure solvent D_{AA} is known, the mutual diffusion coefficient for the solute B in solvent A, D_{AB}, can be related to D_{AA} by Eq(35):

$$\frac{D_{AB}}{D_{AA}} = \exp\ [0.5\delta] \qquad (37)$$

The ratio of mutual to self-diffusion in a particular solvent according to the Stokes-Einstein equation is:

$$\frac{D_{AB}}{D_{AA}} = \frac{r_A}{r_B} \qquad (38)$$

Data for a series of solutes in liquid silver(40,41,42) is presented in Table 1. Here the Stokes-Einstein estimate using Goldschmidt ionic radii of the diffusing solute and solvent molecules shows better agreement with the data than the same estimate using atomic radii.

Diffusivity of Uranium in Liquid Metals

Figures 11 and 12 present diffusivity data for uranium in bismuth, zinc, cadmium and aluminum. Data for all four systems were obtained by Hesson, Hootman, and Burris.(43) The aluminum data of Mitamura(44) are also included. The modified absolute rate theory of Eqs(32) and (33) shows a better agreement with the data than the Stokes-Einstein equation (36), although except for bismuth, both prediction methods are high.

Diffusivity of the Rare Earths in Molten Uranium

The extraction of rare earth fission products from uranium fuel is an important part of some liquid metal

Table 1. Comparison of Calculated and Experimental Mutual to Self-Diffusion Coefficient Ratios for Various Solutes in Silver at 1200°C

	D_{AB}/D_{AA}			
			Stokes-Einstein (Eq. 38)	
Solute in Silver	Exp.[a]	Modified Absolute Rate (Eq. 37)	using Atomic Radii[b]	using Ionic Radii[b]
Gold	0.97	0.90	1.00	0.82
Tin	1.32	1.26	0.91	1.53
Indium	1.35	1.36	0.92	1.23
Antimony	1.37	1.23	0.90	1.26

[a] From equations representing data (40,41,42).

[b] Taken from C. Smithell's "Metals Reference Book", 4th Ed., Plenum (1967).

reprocessing schemes. It is therefore desirable to have available data for the diffusivity of rare earth metals in molten uranium. The only data in the literature are those of Smith(45) who measured the diffusivity of cerium in uranium over the temperature range 1170-1480°C. The experiments were carried out in fairly large tantalum crucibles (7 mm. diameter). According to the author, convection at the higher temperatures due to the large diameter increased the uncertainty of the results in the range 1400-1480°C. The value determined at the melting point of uranium, $D=8.8 \times 10^{-5}$ cm^2/sec, seems somewhat high also. The value calculated by the Stokes-Einstein equation is 1.5×10^{-5} cm^2/sec. The modified absolute rate method gives 2.5×10^{-5} cm^2/sec.

The modified absolute rate method for calculating diffusivities is convenient to use since it requires only viscosity data for the pure solvent and pure solute. The Stokes-Einstein equation involves an uncertainty as to the correct radius to assign the diffusing solute atom, although most workers use the ionic radius. In general, the modified absolute rate method is more accurate. When applied to common binary metal systems, the Fig. 10 experimental data are correlated to within ±25%. For uranium as solute, good agreement is obtained only with bismuth. The 50% discrepancy in zinc, cadmium and aluminum may indicate that the diffusing amount is larger than a single uranium atom, and may be an intermetallic compound of uranium and the solvent.

Measurement of Liquid Metal Transport Properties

The measurement of the coefficients of viscosity and diffusivity in liquid metals is subject to the same experimental problems as the mass transfer studies discussed earlier. Because of the high temperatures involved, construction material and equipment complexity are severely restricted (at least within the hot zone of the furnace). The generation of a prescribed flow field in the liquid metal is all-important in both viscosity and diffusivity measurements. In the former, the fluid mechanics of the device must be known because the relation between the shear stress and velocity gradients in the fluid establishes the coefficient of viscosity. In diffusion measurements, all fluid velocities should be zero.

Viscosity

The various methods which have been used to measure liquid metal viscosities have been reviewed by Thresh(46).

In the capillary method, the liquid is forced through a narrow tube by inert gas pressure or by the hydrostatic head of the moving fluid itself. The use of an inert gas is often incompatible with the vacuum system required to insure fluid cleanliness. Surface tension effects may inhibit flow in the capillary. A rather large hot zone is necessary and the mechanical complexity of the open flow renders this method unsuitable for high melting reactive metals.

In rotational viscometers, the liquid metal is contained as an annular ring formed by a central cylinder rotating at a constant speed and a stationary outer cylinder. The viscosity can be determined by the torque on the outer cylinder. The problems of driving the inner cylinder and of measuring the torque on the outer cylinder are difficult in high temperature vacuum systems. In addition, accumulation of slag (due to impurities) at the rather small annular liquid surface between the two cylinders significantly affects the measurements.

Oscillating crucible viscometers have been used almost exclusively for viscosity measurements above 1000°C. In this method, a specimen of metal is sealed in a cylindrical crucible suspended in the hot zone of a furnace by a torsion wire. The pendulum is given an initial twist and the damping of the torsional oscillations is directly related to the viscosity. The amount of metal used is quite modest: specimens are ∿ 2 cm diameter by ∿ 7 cm high, and of an easily machinable shape. The simple geometry also permits fabrication of nearly any high temperature container material for the crucible. The crucible (or an outer refractory metal sheath) can be vacuum sealed by electron beam welding, thereby permitting complete isolation of the melt from the vacuum environment and attainment of temperatures at which the vapor pressure of the liquid would otherwise be unacceptably high for the vacuum system. The only motion required is simple torsional oscillation, which can be initiated from outside the vacuum system. No measurements within the vacuum system are required; the temperature can be measured with an optical pyrometer and the period and damping constant of the oscillation are determined by the motion of a light beam reflected from the part of the pendulum outside of the furnace. The liquid metal surface is relatively large (∿ 2 cm diameter), thereby reducing the effects of surface tension and slag-wall interactions.

The apparatus depicted in Fig. 13 is currently in use in our laboratory, but is typical of the design of most high temperature vacuum oscillating crucible viscometers.

The furnace heater element (A) is surrounded by a series of tungsten radiation shields (B). The entire system is contained within a vacuum system (C).

The torsion pendulum consists of three primary parts: the crucible (D) which contains the metal specimen; a rod (E) which rigidly connects the crucible with the part of the pendulum outside of the hot zone; and the external portion of the pendulum (F) which has a polished surface to reflect a beam of light by which the motion of the pendulum is monitored. A hole is drilled through the pendulum perpendicular to its axis of rotation into which rods may be inserted and fixed such that the moment of inertia of the pendulum may be varied. The small chuck at (G) attaches the pendulum to the torsion wire. A picture of the entire pendulum in shown in Fig. 14.

The torsion wire (H) extends from the pendulum to a second chuck which is attached to a rotatable holder (J) which rests on a support plate (K). The holder is attached mechanically to a rotary feedthrough (L) by which the rotary motion of the pendulum may be initiated from outside the vacuum system.

The temperature within the furnace region is measured by an optical pyrometer (M) which is sighted through a right angle prism (N) into a hole, 1/8 inch in diameter, drilled through the bottom shield pack into the inner furnace region.

Diffusion Coefficients

Most liquid metal diffusivity measurements are performed in "capillary" cells. In room temperature measurements on aqueous or organic solutions, diffusion occurs along the length of narrow bore tubing, and the concentration profile can be directly measured by optical methods. With liquid metals, however, the capillary is more aptly described as a tube, since diameters up to 7 mm have been used. The concentration profile cannot be measured *in situ*; rather the final profile is determined by freezing the system and sectioning the capillary for analysis by chemical or radiochemical means. Application of the common capillary methods to liquid metals has been discussed by Niwa et al(47).

For low melting metals, a U-tube containing the pure solvent is lowered into an alloy bath. After a definite diffusion time, the U-tube is withdrawn from the bath, quenched and sectioned for analysis. Because of the very uniform temperature of the alloy bath into which the U-tube is placed, temperature variations and the resulting natural convection in the diffusion region are virtually eliminated. However, the method is inconvenient for high temperature vacuum environments because of the rather substantial amount of metal required for the alloy bath and because of the complications involved in raising and lowering the U-tube into and out of the hot zone.

The bath-less capillary method utilized by Smith(45) for measurements of diffusion in uranium is suitable for reactive liquid metals at temperatures above 1000°C. Smith's apparatus is shown in Fig. 15. In this arrangement, both components are placed in the cylindrical crucible which serves as the diffusion "capillary". Care must be taken to avoid convective mixing of the two components (which may or may not be immiscible when liquid) during melting. This method is more susceptible to natural convection mixing due to temperature gradients than is the bath method. Natural convection can be reduced by using specimens of large length-to-diameter ratios, although this geometry accentuates the effect of gettering of the diffusing solute by reaction with the container wall. The effects of vertical and horizontal temperature gradients on induced convective motion have been analyzed by Verhoeven(48) and found to be an unlikely source of systematic error (theoretically at least). The mixing which occurs during melting and freezing of the sample, however, can undoubtedly contribute to high apparent diffusion coefficients.

This work was supported by the United States Atomic Energy Commission.

References

1. ANL 7548, p. 109 (1969).

2. Dunn, W.E., C.F. Bonilla, C. Ferstenberg, and B. Gross, A.I.Ch.E. Journal, 2, 184 (1956).

3. Kassner, T.F., J. Electrochem. Soc., 114, 689 (1967).

4. Sideman, S. and H. Shabtai, Can. J. Chem. Eng., 42, 107 (1964).

5. Higbie, R., Trans. Am. Inst. Chem. Engrs., 31, 365 (1935).

6. Newman, A.B., Trans. Am. Inst. Chem. Engrs., 27, 203 (1931).

7. Kronig, R. and J.C. Brink, Appl. Sce. Res., A2, 142 (1950).

8. Handlos, A.E. and T. Baron, A.I.Ch.E. Journal 3, 129 (1957).

9. Angelo, J.B., E.N. Lightfoot and D.W. Howard, A.I. Ch.E. Journal, 12, 751 (1966).

10. Rose, D.M. and R.C. Kintner, A.I.Ch.E. Journal, 12, 530 (1966).

11. Olander, D.R., A.I.Ch.E. Journal, 12, 1018 (1966).

12. Patel, J.M. and R.M. Wellek, A.I.Ch.E. Journal, 13, 384 (1967).

13. Pasternak, A.D., UCRL-16108 (1966).

14. Hu, C. and R.C. Kintner, A.I.Ch.E. Journal, 1, 42 (1955).

15. Bonilla, C.F., First Int'l Conf. on Peaceful Uses of At. Energy, United Nations, Geneva, 9, paper no. 122, pp. 331-40 (1955).

16. Katz, H.M., F.B. Hill and J.L. Speirs, Trans. Met. Soc. AIME, 218, 770 (1960).

17. Olander, D.R., Nuc. Sci. Eng., 31, 1 (1968).

18. Pasternak, A.D. and D.R. Olander, A.I.Ch.E. Journal, 14, 235 (1968).

19. Grosse, A.V., J. Inorg. and Nucl. Chem., 25, 317 (1963).

20. Chapman, T.W., A.I.Ch.E. Journal, 12, 395 (1966).

21. Andrade, E.E., Phil. Mag., 17, 698 (1934).

22. Andrade, E.W., Phil. Mag., 17, 497 (1934).

23. Jones, L.V., D. Ofte, W.G. Rohr, and L.J. Wittenberg, Trans. of the ASM, 55, 819 (1962).

24. Ofte, D., J. Nucl. Mater. 22, 28 (1967).

25. Finucane, J. and D. Olander, unpublished data.

26. Wittenberg, L.J., D. Ofte, and W.G. Rohr, Rare Earth Research, Vol. II, ed. by K.S. Vorres, Gordon and Breach, New York, 1964, pp. 257-275.

27. Rohr, W.G., J. Less-Common Metals, 10, 389 (1966).

28. Ofte, D., W.G. Rohr, and L.J. Wittenberg, Plutonium 1965, Proc. of the 3rd Internat'l Conf. on Plutonium, London, 1965, ed. by A.E. Kay and M.B. Waldron, Chapman and Hall, London (1965), pp. 405-419.

29. Ofte, D. and L.J. Wittenberg, Trans. ASM, 57, 917 (1964).

30. MLM-1402, Reactor Fuels and Materials Development Plutonium Research: 1966 Annual Report, October 16, 1967, pp. 40-44.

31. Ofte, D. and W.G. Rohr, J. Nucl. Mater., 15, 231 (1965).

32. Fisher, H.J. and A. Phillips, J. of Metals, 1060 (1954).

33. Kanda, F.A. and R.P. Colburn, Phys. and Chem. of Liquids, 1, 159 (1968).

34. Burylev, B.P. translated in Russian Journal of Physical Chemistry, 41, 53 (1967).

35. Eretnov, K.I. and A.P. Lyubimov, Ukr. Ziz. Zhur., 12, 214 (1967).

36. Gvozdeva, L.I. and A.P. Lyubimov, Ukr. Ziz. Zhur., 12, 208 (1967).

37. Pasternak, A.D. and D.R. Olander, A.I.Ch.E. Journal, 13, 1052 (1967).

38. Olander, D.R., A.I.Ch.E. Journal, 9, 207 (1963).

39. Glasstone, S., K.J. Laidler, and H. Eyring, Theory of Rate Processes, McGraw-Hill, New York (1941).

40. Swalin, R.A. and V.G. Leak, Acta. Met., 13, 471 (1966).

41. Gupta, Y.P., Acta. Met., 14, 297 (1966).

42. Leak, V.G. and R.A. Swalin, Trans. Met. Soc. AIME, 230, 426 (1964).

43. Hesson, J.C., H.E. Hootman, and L. Burris, Jr., J. Electrochem. Tech., 3, 240 (1965).

44. Mitamura, N. Nippon Genshiryoku Gakkaishi, 5, 467 (1963). (Data from NSA 17, 32500).

45. Smith, T., J. Electrochem. Soc., 106, 1046 (1959).

46. Thresh, H.R., Trans. ASM, 55, 790 (1962).

47. Niwa, K., M. Shimaji, S. Kado, Y. Watanabe, and T. Yokukawa, Trans. AIME, 209, 96 (1957).

48. Verhoeven, J.E., Trans. AIME, 242, 1937 (1968).

List of Figures

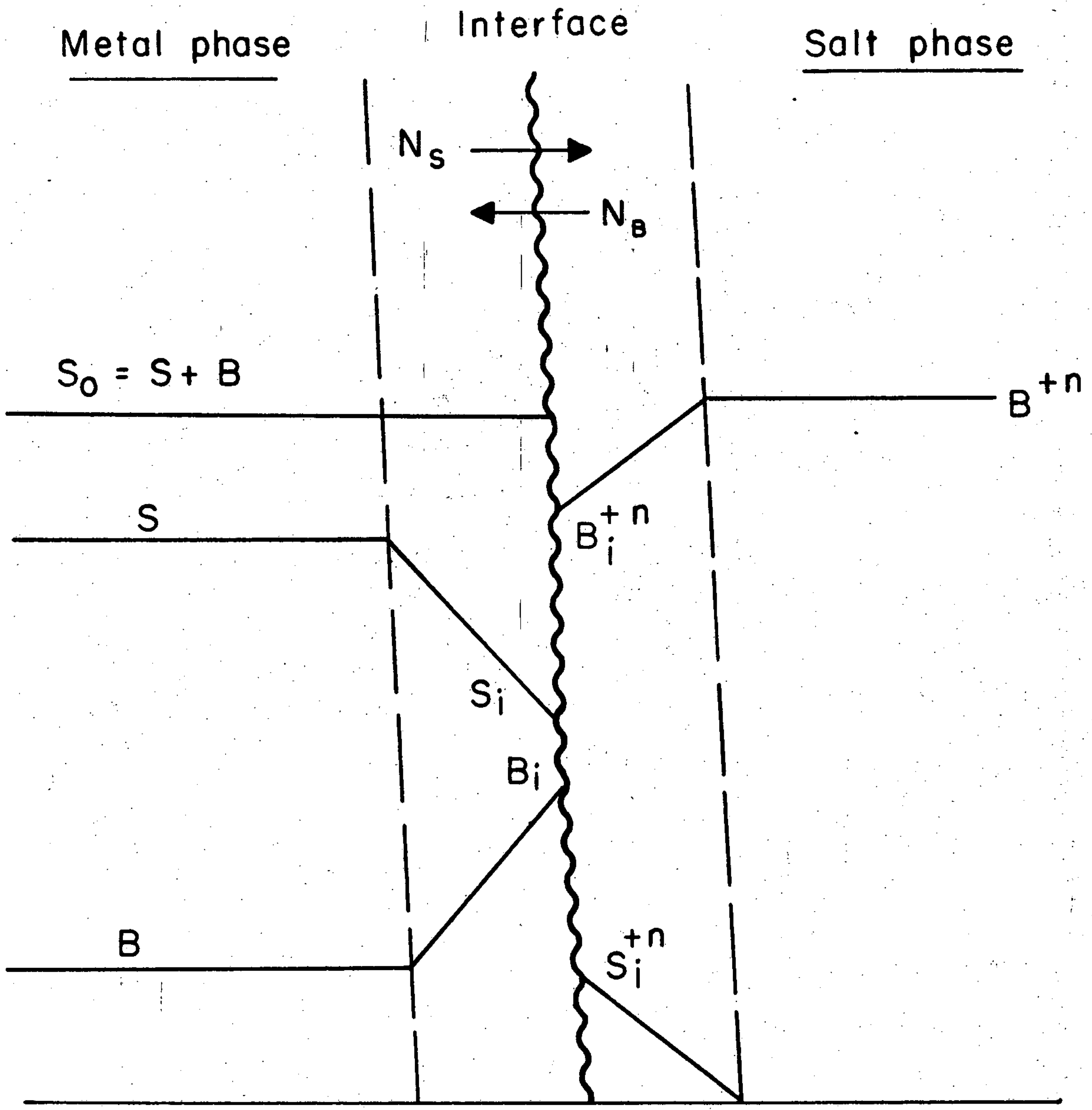

XBL694-2588

Fig. 1

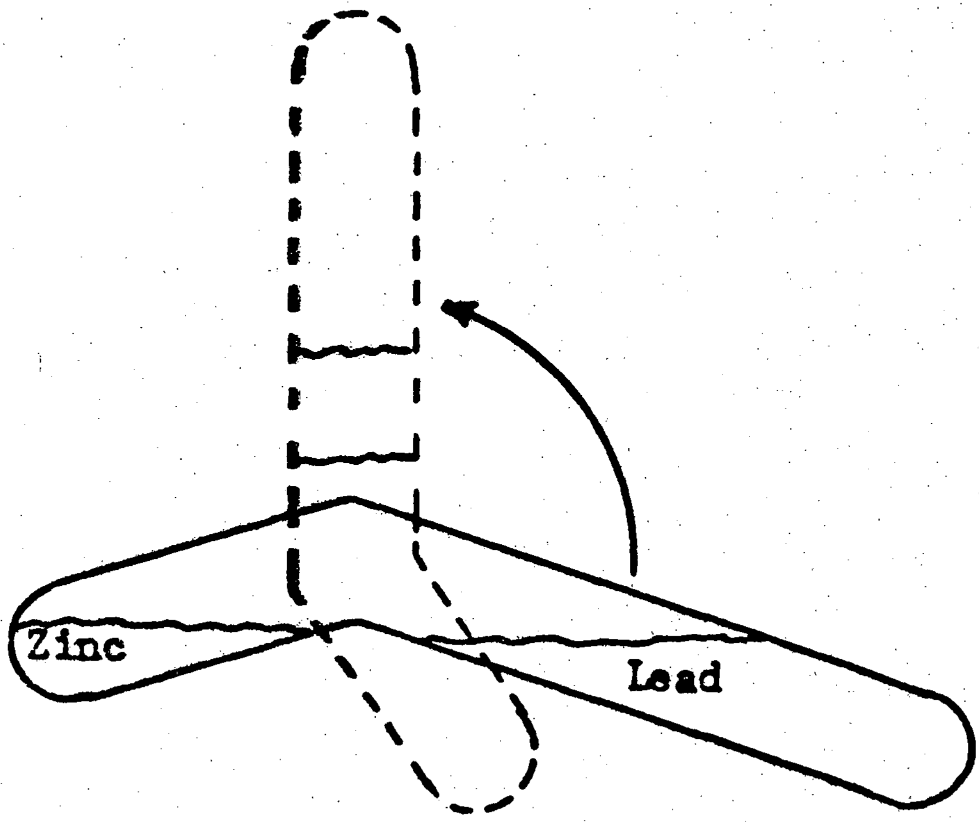

XBL 694-445

Fig. 2

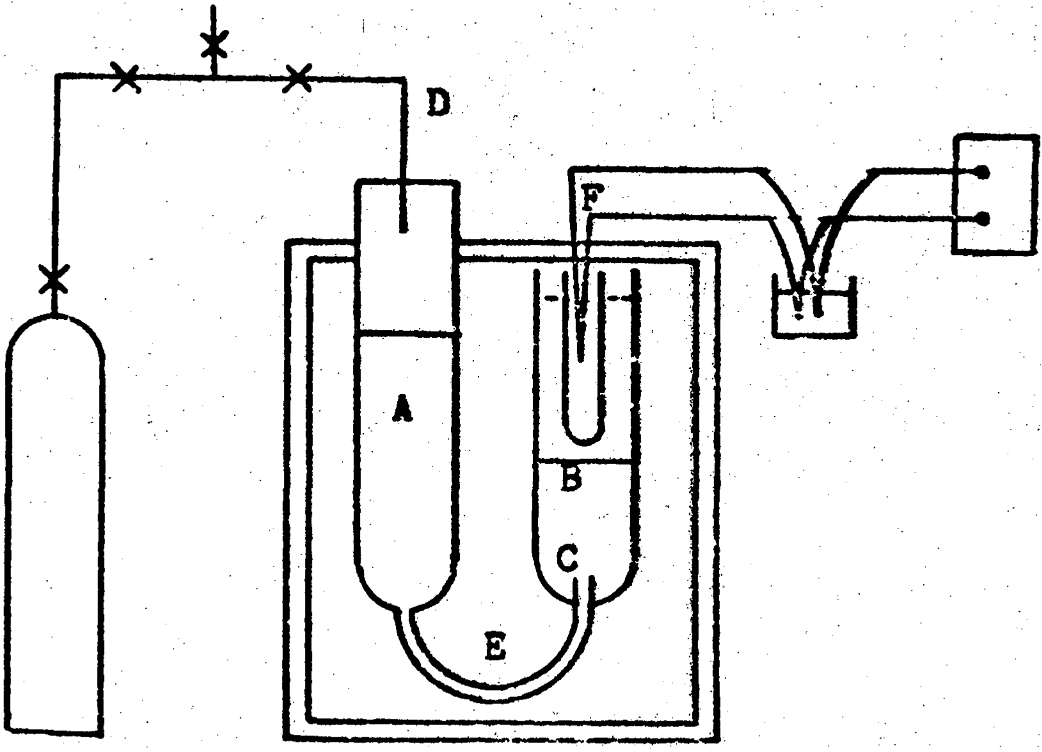

XBL 694-442

Fig. 3

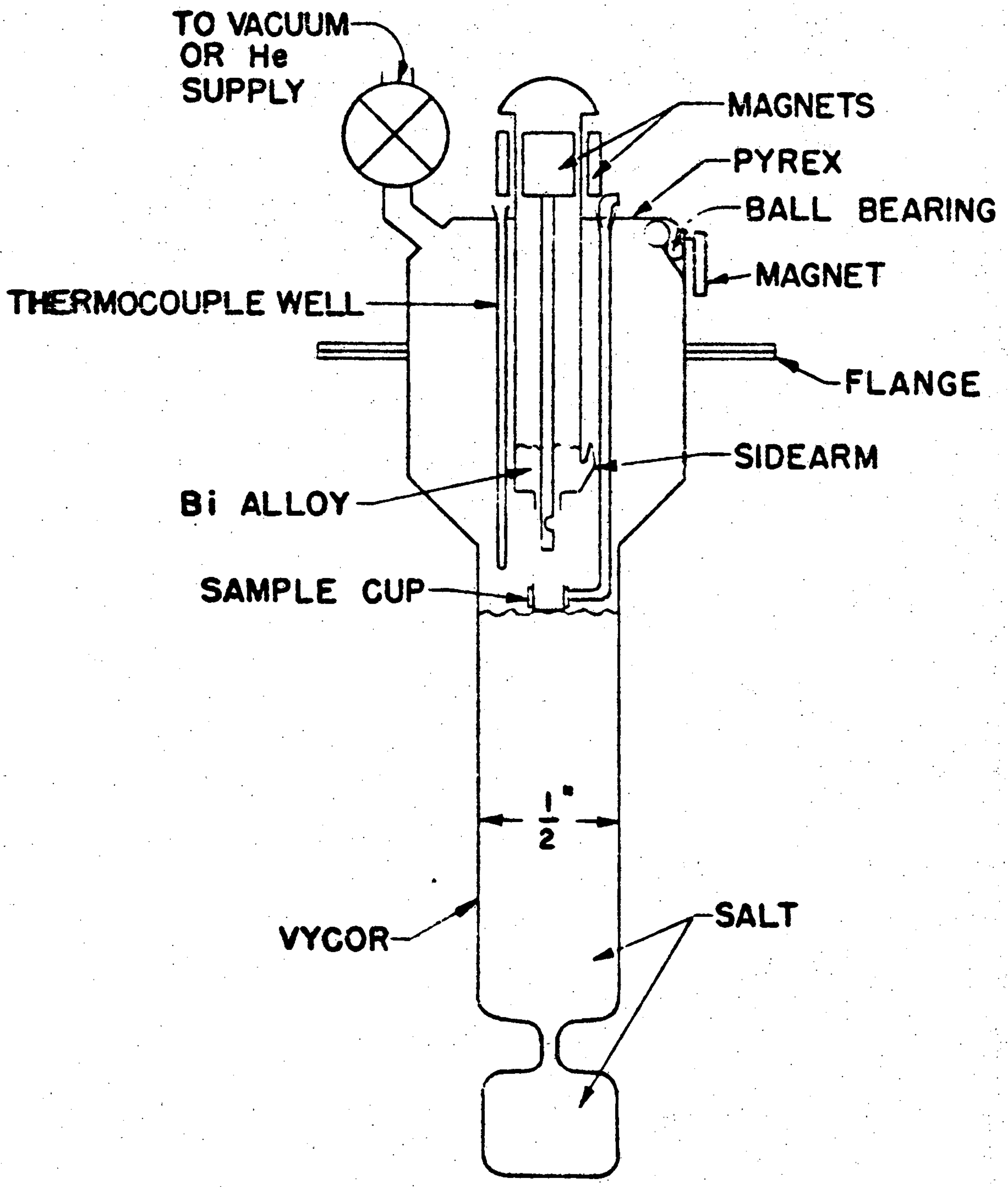

XBL 694-444

Fig. 4

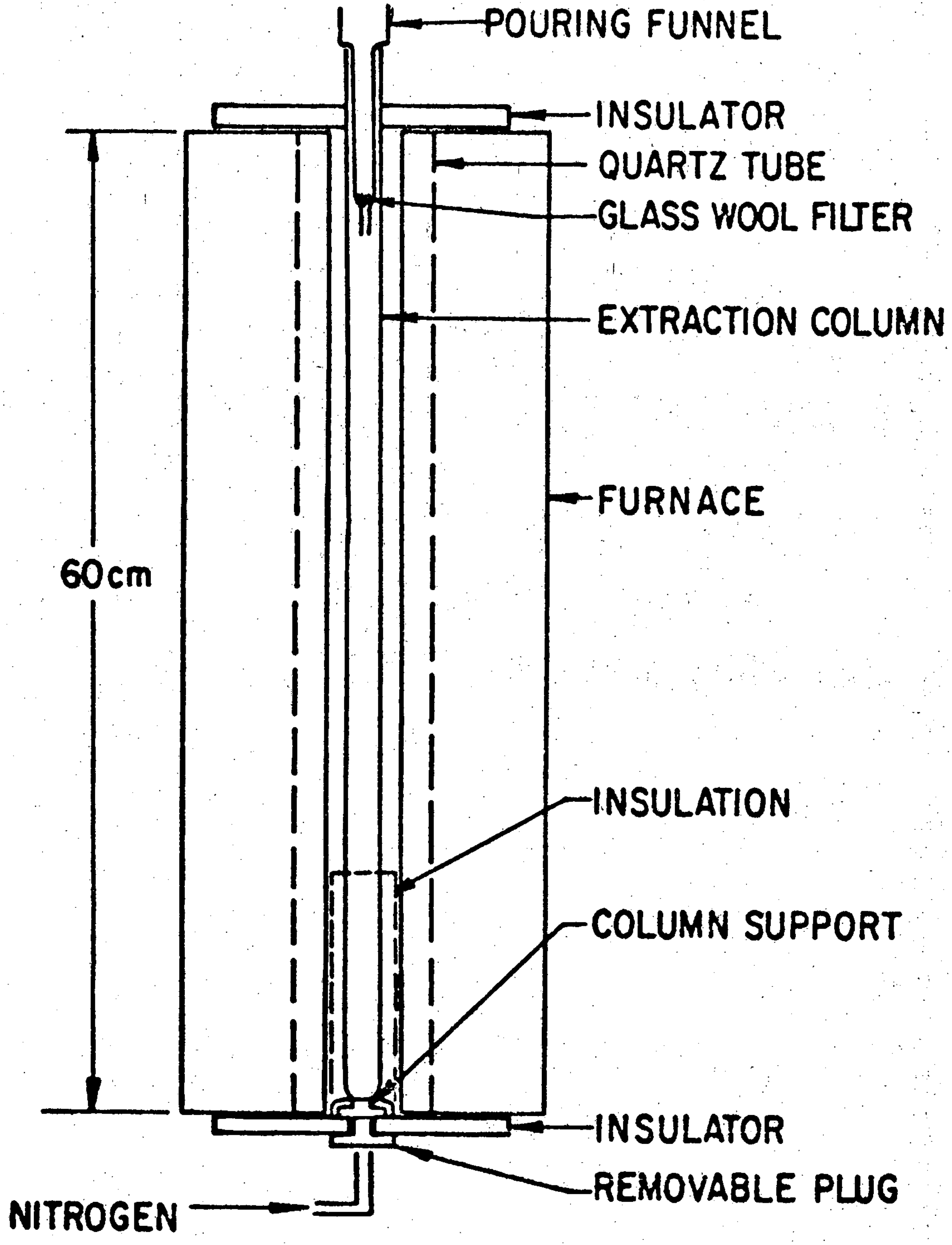

XBL 694-443

Fig. 5

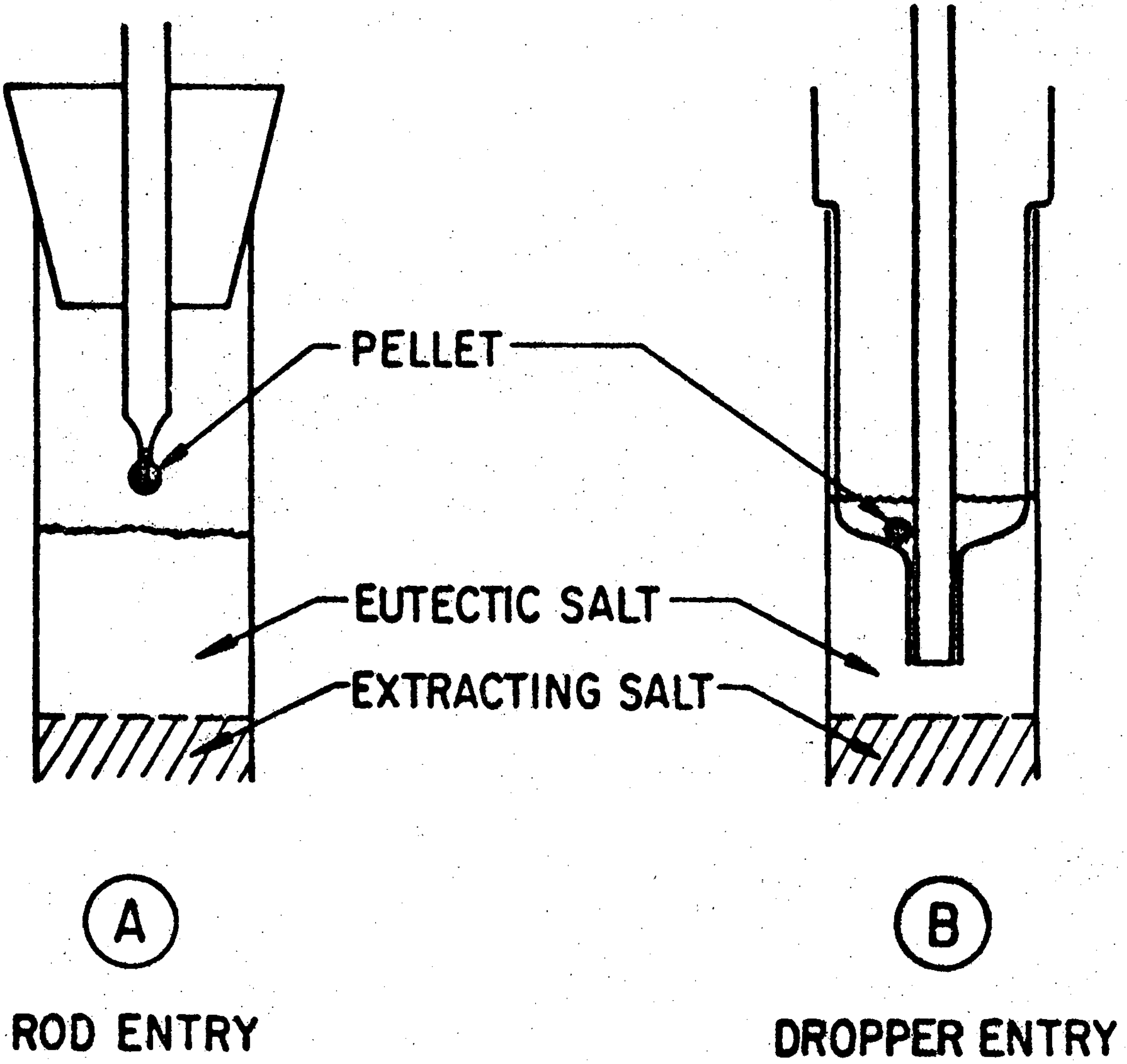

XBL 694-446

Fig. 6

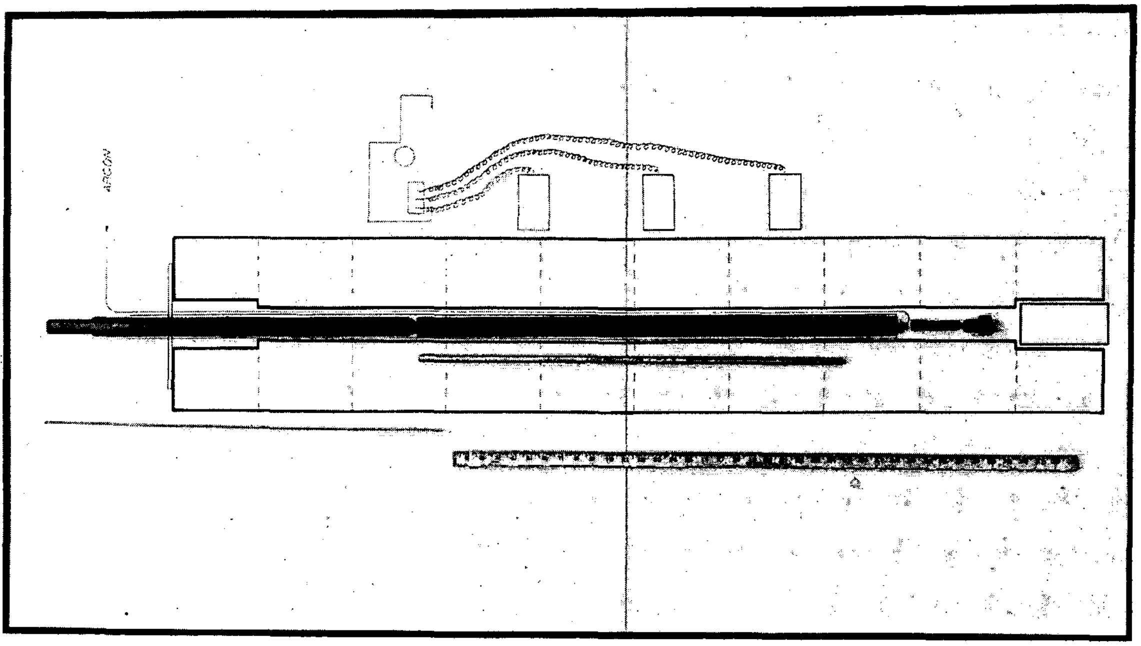

IM 1831

Fig. 7

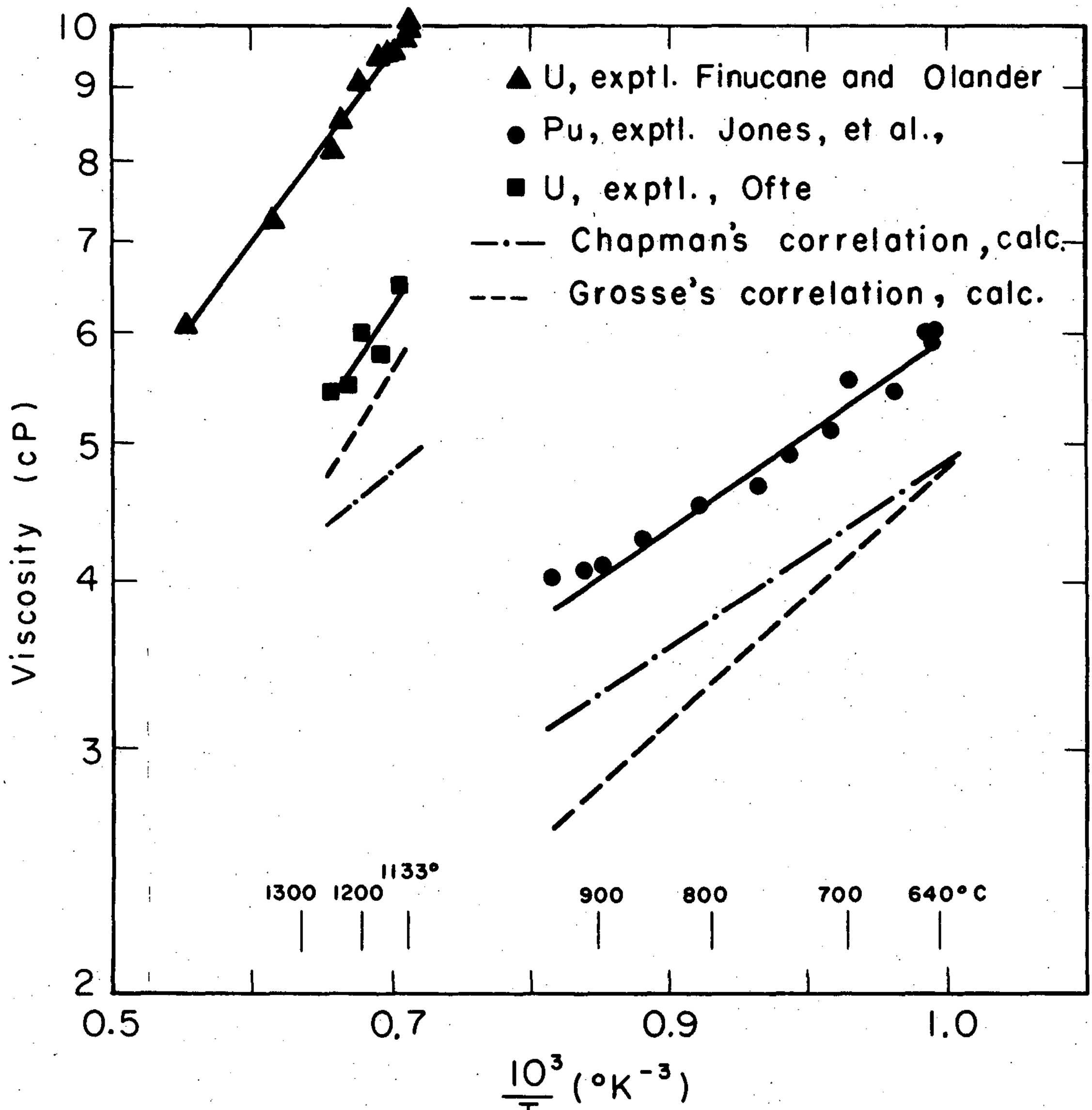

XBL694-2609

Fig. 8

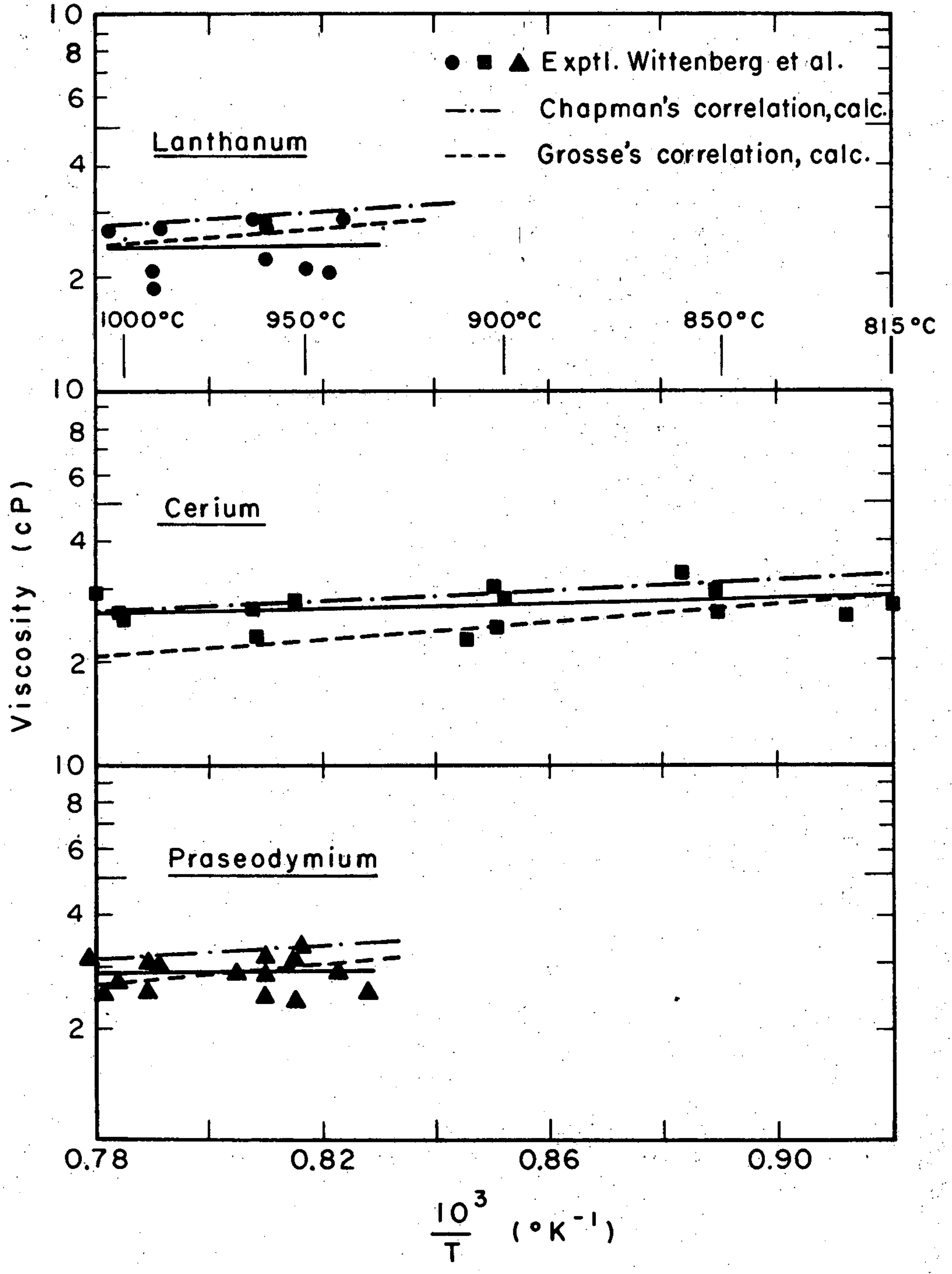

XBL694-2589

Fig. 9

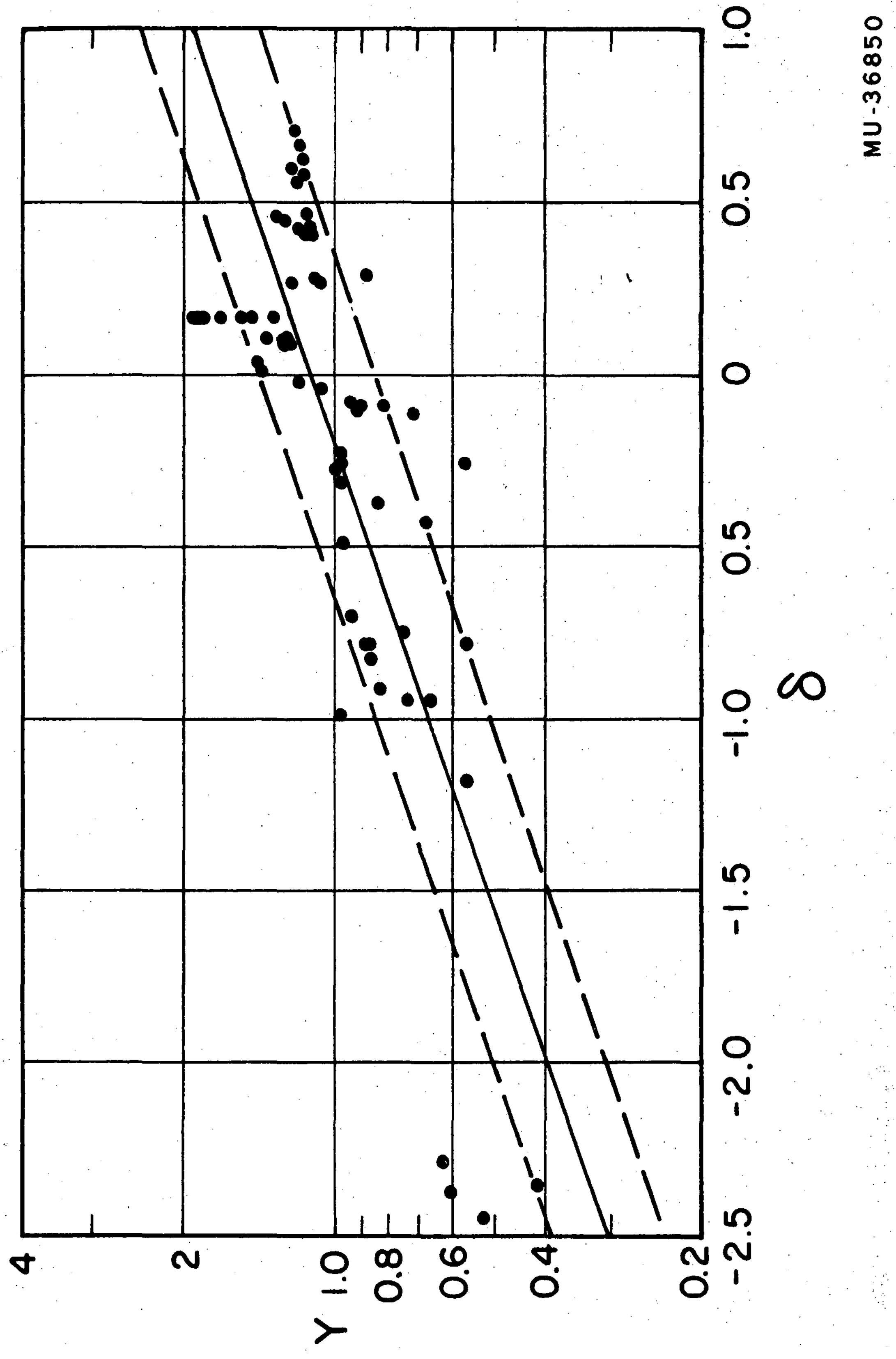

Fig. 10

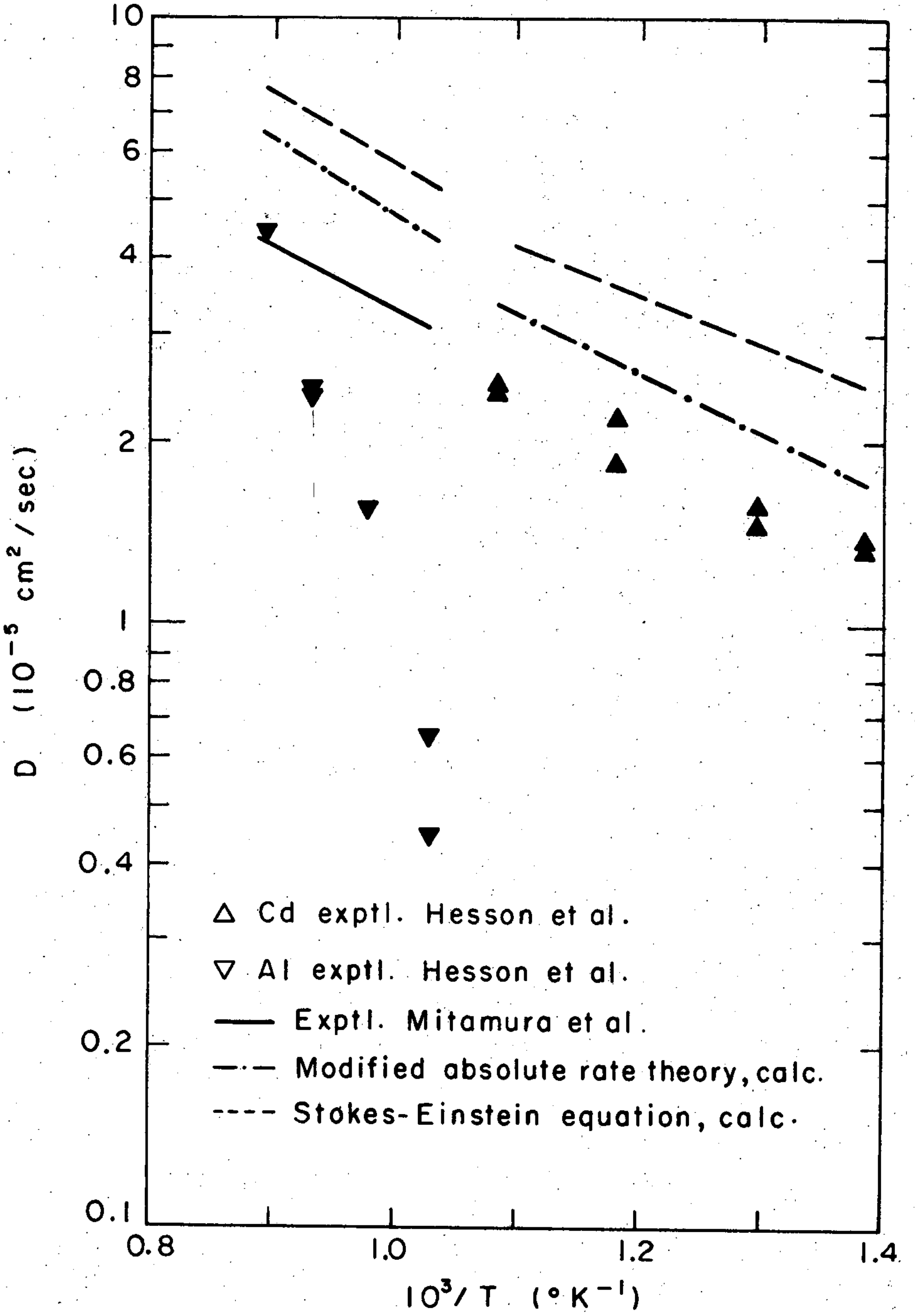

XBL694-2590

Fig. 11

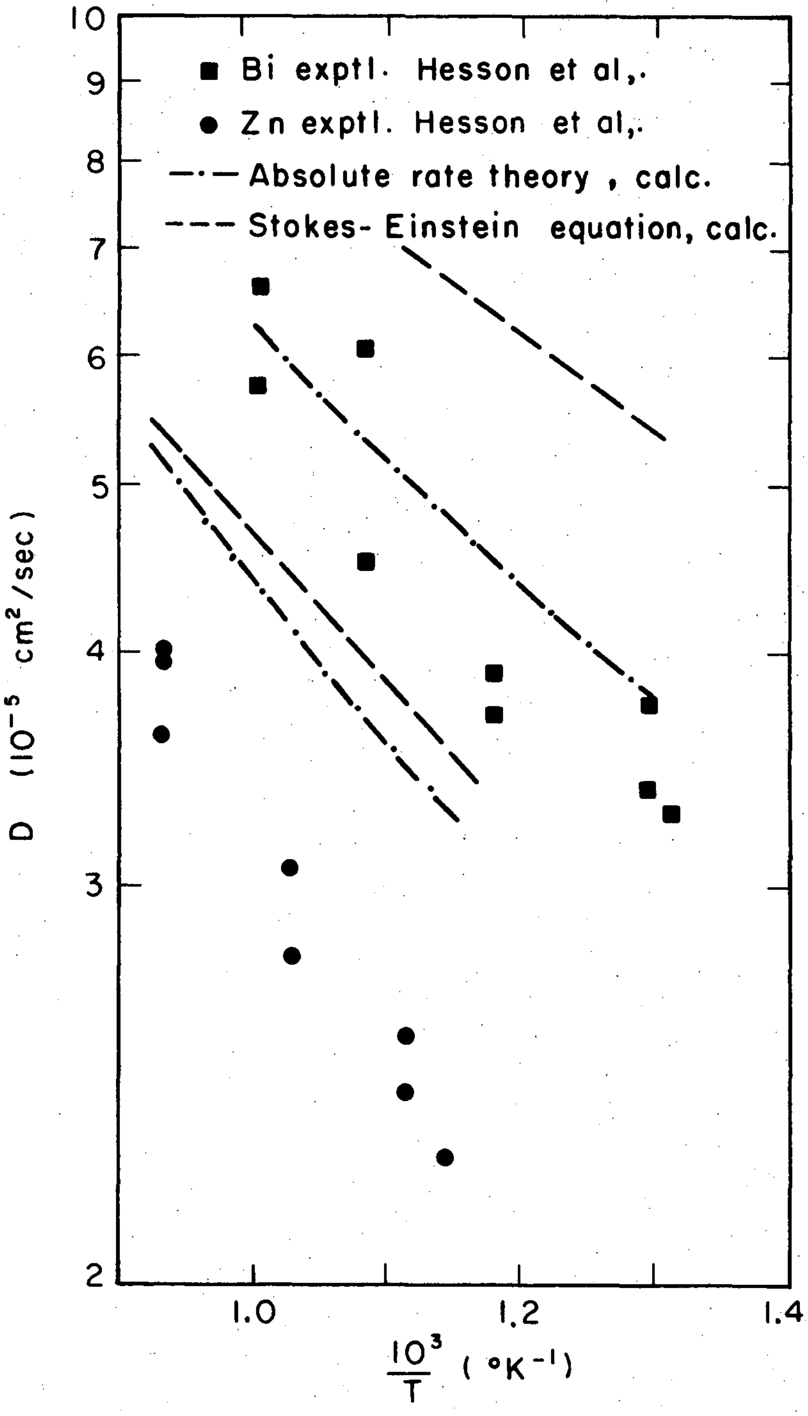

XBL694-2591

Fig. 12

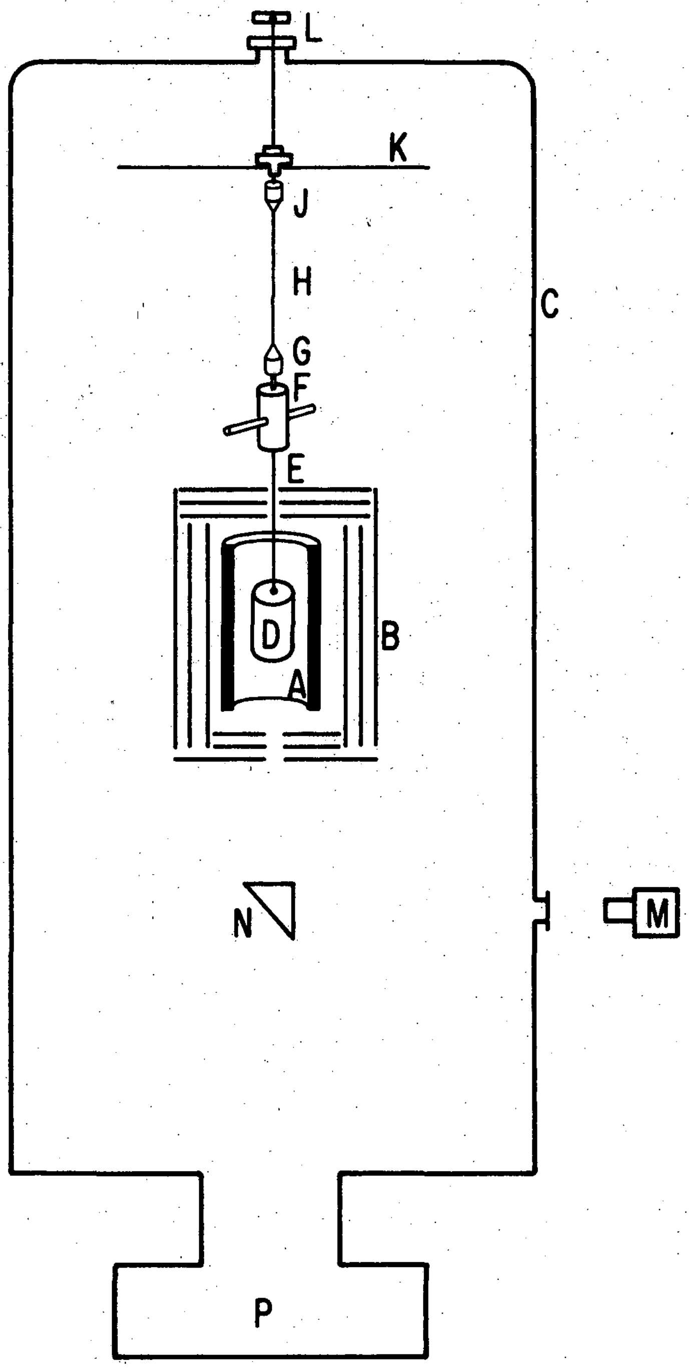

XBL 694-426

Fig. 13

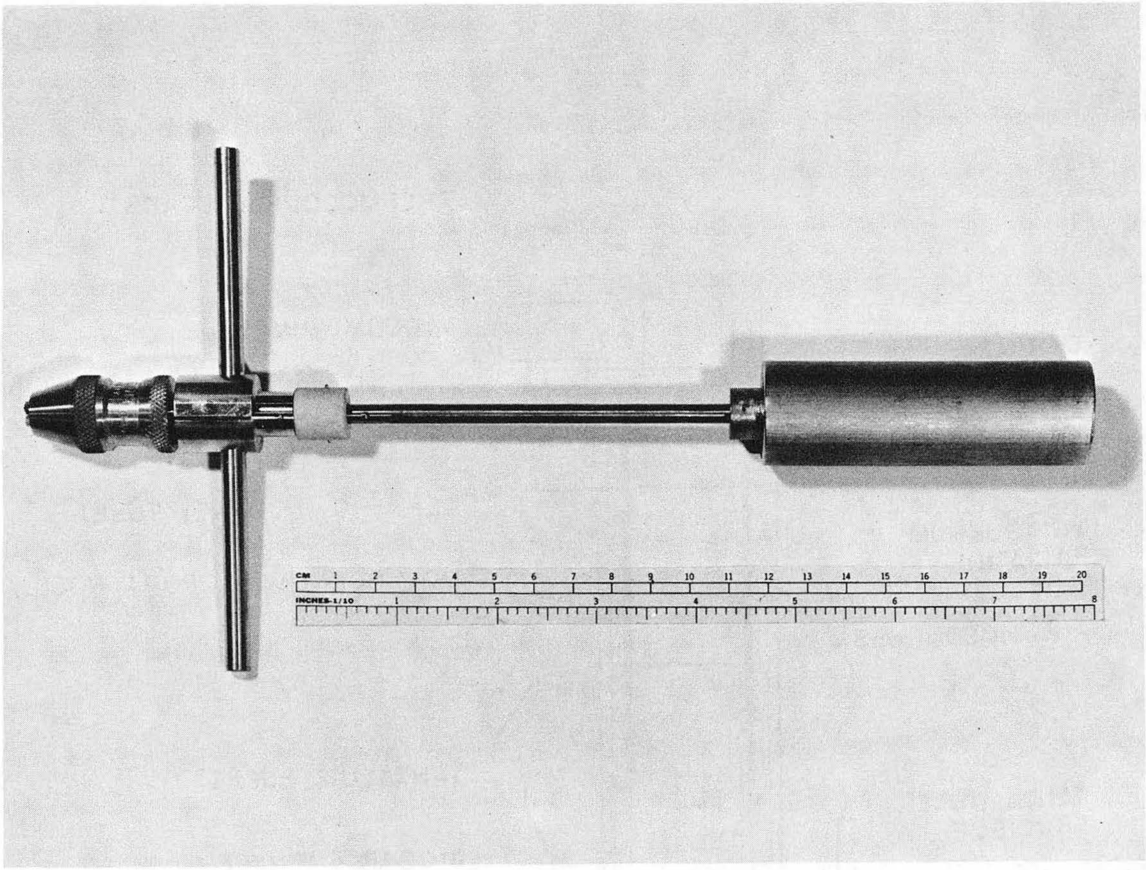

XBB 6811-6906

Fig. 14

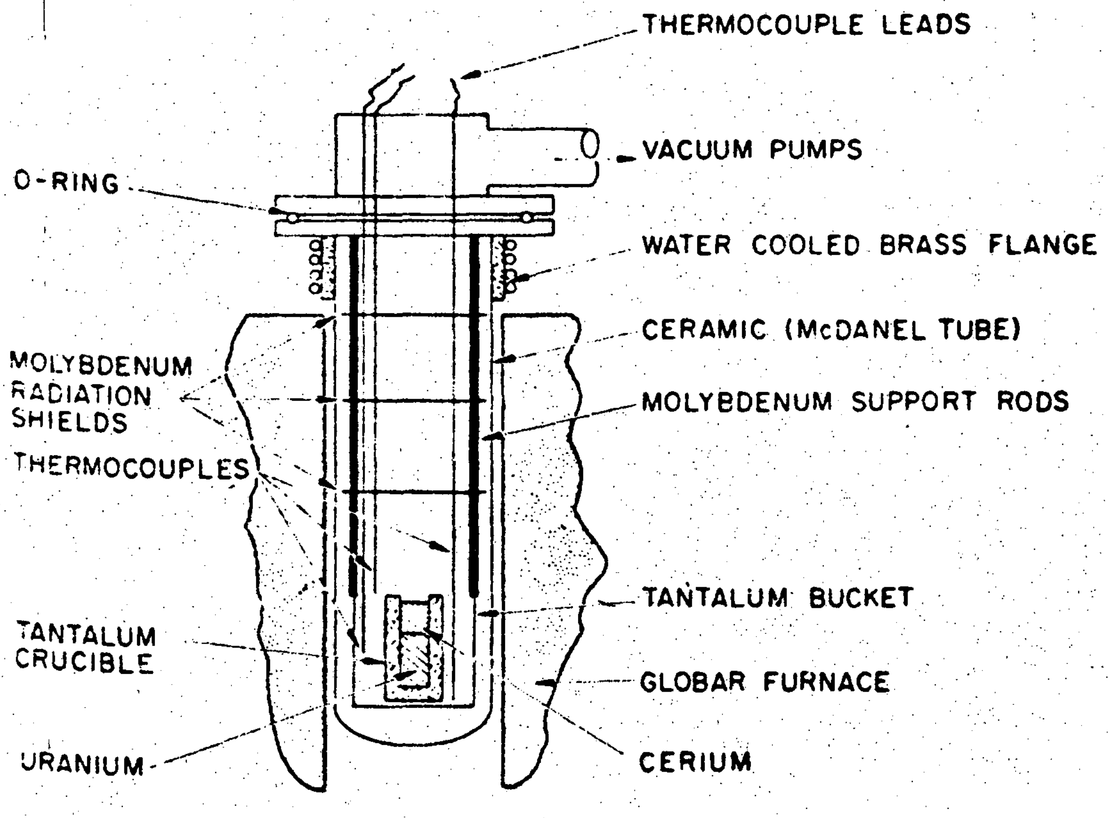

XBL 694-441

Fig. 15

TECHNICAL INFORMATION DIVISION
LAWRENCE RADIATION LABORATORY
UNIVERSITY OF CALIFORNIA
BERKELEY, CALIFORNIA 94720